THE FASEB JOURNAL • RESEARCH • www.fasebj.org

Complement-induced activation of MAPKs and Akt during sepsis: role in cardiac dysfunction

Fatemeh Fattahi,[*,1] Miriam Kalbitz,[†,1] Elizabeth A. Malan,[*] Elizabeth Abe,[*] Lawrence Jajou,[*] Markus S. Huber-Lang,[†] Markus Bosmann,[‡] Mark W. Russell,[§] Firas S. Zetoune,[*] and Peter A. Ward[*,2]

[*]Department of Pathology and [§]Department of Pediatrics and Communicable Diseases, University of Michigan Medical School, Ann Arbor, Michigan, USA; [†]Department of Orthopaedic Trauma, Hand, Plastic, and Reconstructive Surgery, University Hospital of Ulm, Ulm, Germany; and [‡]Center for Thrombosis and Hemostasis, University Medical Center, Mainz, Germany

ABSTRACT: Polymicrobial sepsis in mice causes myocardial dysfunction after generation of the complement anaphylatoxin, complement component 5a (C5a). C5a interacts with its receptors on cardiomyocytes (CMs), resulting in redox imbalance and cardiac dysfunction that can be functionally measured and quantitated using Doppler echocardiography. In this report we have evaluated activation of MAPKs and Akt in CMs exposed to C5a *in vitro* and after cecal ligation and puncture (CLP) *in vivo*. In both cases, C5a *in vitro* caused activation (phosphorylation) of MAPKs and Akt in CMs, which required availability of both C5a receptors. Using immunofluorescence technology, activation of MAPKs and Akt occurred in left ventricular (LV) CMs, requiring both C5a receptors, C5aR1 and -2. Use of a water-soluble p38 inhibitor curtailed activation *in vivo* of MAPKs and Akt in LV CMs as well as the appearance of cytokines and histones in plasma from CLP mice. When mouse macrophages were exposed *in vitro* to LPS, activation of MAPKs and Akt also occurred. The copresence of the p38 inhibitor blocked these activation responses. Finally, the presence of the p38 inhibitor in CLP mice reduced the development of cardiac dysfunction. These data suggest that polymicrobial sepsis causes cardiac dysfunction that appears to be linked to activation of MAPKs and Akt in heart.—Fattahi, F., Kalbitz, M., Malan, E. A., Abe, E., Jajou, L., Huber-Lang, M. S., Bosmann, M., Russell, M. W., Zetoune, F. S., Ward, P. A. Complement-induced activation of MAPKs and Akt during sepsis: role in cardiac dysfunction. FASEB J. 31, 4129–4139 (2017). www.fasebj.org

KEY WORDS: CLP · cardiomyocyte · C5a receptor

In humans, sepsis often leads to myocardial dysfunction in at least 40% of patients, and it has been associated with mortality rates as high as 70% (1–3). In rodents and humans, activation of the complement system during sepsis results in robust production of the complement anaphylatoxin, complement component 5a (C5a) (4), at levels that correlate with the severity of sepsis (5). Absence or blockade of either C5a receptor (C5aR) substantially improved survival rates in mice after cecal ligation and puncture (CLP)-induced sepsis (6). Addition of recombinant C5a to rat or mouse cardiomyocytes (CMs) caused CM dysfunction, involving both contractility and relaxation (7, 8). Likewise, CMs isolated from CLP hearts showed increased levels of C5aR1 (8). These data suggest that C5a plays an important role in the development of harmful outcomes of sepsis, especially involving the heart, through its receptors (C5aR1 and -2) on CMs (9).

Interaction of C5a with its receptors leads to many pleiotropic effects, including the release of cytokines and chemokines and recruitment of inflammatory cells (10). In certain circumstances, C5a-C5aR interactions can also result in the activation of signaling pathways in CMs including MAPKs, which in turn modulate transcriptional factors that amplify gene expression (11). There are 3 well-defined MAPK pathways: ERK-1/2, JNK-1/2, and p38 (12). MAPK signaling efficiency and specificity are modulated by protein–protein interactions between individual MAPKs and the docking motifs in cognate binding partners (13). Important signaling pathways regulating responses of the cells to the infection and stress are *via* MAPKs (14). MAPKs have emerged in many cell types as important signaling pathways in a variety of biologic processes, such as inflammation, cell growth, cell differentiation, cell cycle, and

ABBREVIATIONS: C5a, complement component 5a; C5aR, complement component 5a receptor; CLP, cecal ligation and puncture; CM, cardiomyocyte; E/A, E-wave (early)/A-wave (late) diastolic filling velocity; echo Doppler, Doppler echocardiography; IC_{50}, half maximum inhibitory concentration; I/R, ischemia–reperfusion; IVRT, isovolumic relaxation time; KO, knockout; LV, left ventricular; MAPKAPK, MAPK-activated protein kinase; MV, mitral valve; PEM, peritoneal exudate macrophage; rrC5a, recombinant rat C5a; TnT, troponin-T; WT, wild type

[1] These authors contributed equally to this work.

[2] Correspondence: Department of Pathology, University of Michigan Medical School,1301 Catherine Rd., 7520 MSRB I, Box 5602, Ann Arbor, MI 48109-5602, USA. E-mail: pward@umich.edu

doi: 10.1096/fj.201700140R

This article includes supplemental data. Please visit *http://www.fasebj.org* to obtain this information.

cell death and during ischemia–reperfusion (I/R) injury, sepsis, and many other diseases (15, 16).

In the heart, I/R injury and ischemic heart failure has been shown to activate signaling cascades of the MAPK family (17, 18). Once activated, MAPKs phosphorylate several downstream targets (other protein kinases and transcription factors) (16). The activation of MAPKs has been proposed to be initially mediated *via* the activation of members of the Src family tyrosine kinases through a Shc/Grb2/Ras signaling cascade (17). In addition to MAPK, Ras-GTP has been shown to bind and activate PI3K (17, 19). PI3K activation phosphorylates and activates downstream of a serine/threonine-specific protein kinase called Akt (also known as PKB). Akt is activated by a variety of growth factors and cellular stresses *via* phosphorylation on threonine 308 (T308) and serine 473 (S473) residues (17).

The coinvolvement of MAPK and Akt signaling pathways has been described in I/R injuries. We found coinvolvement of MAPK and Akt signaling in I/R injury in liver (20). Several other reports showed involvement of both MAPK and Akt signaling pathways in cardiac I/R injury (21–26). To our knowledge, there are few, if any, published reports about the coinvolvement of MAPKs and Akt signaling pathways in cardiac defects after sepsis. In the current study we investigated activation (phosphorylation) of MAPKs (p38, ERK-1/2, and JNK-1/2) and Akt in mouse CMs after CLP or after *in vitro* exposure to C5a. We also used the water-soluble inhibitor of p38 to characterize the linkage between MAPK activation and development of cardiac dysfunction during sepsis.

MATERIALS AND METHODS

Animals

All procedures were performed according to the *Guide for the Care and Use of Laboratory Animals* (National Institutes of Health, Bethesda, MD, USA) and were approved by the University of Michigan Committee on Use and Care of Animals. Specific pathogen-free male Sprague-Dawley rats (300–350 g) (Harlan Laboratories, Indianapolis, IN, USA) and male C57BL/6 mice (8–10 wk, 25–30 g) (The Jackson Laboratories, Bar Harbor, ME, USA) were used in this study. Some experiments were also performed in male C57BL/6 mice from our own C5aR1$^{-/-}$ and C5aR2$^{-/-}$ breeding colonies at the University of Michigan. The generation of C5aR1$^{-/-}$ and C5aR2$^{-/-}$ mice has been described in refs. 27 and 28.

Experimental sepsis

Midgrade CLP (~50% survival after 7 d) was performed in this study, according to a published procedure (29, 30). The animals were euthanized 8, 16, 24, or 48 h after CLP.

Isolation of CMs

The isolation of young adult CMs was performed with rat and mouse hearts (7, 30, 31). After isolation, we increased in a stepwise manner the Ca^{2+} concentrations in the medium, to achieve physiologic levels of Ca^{2+}. These procedures avoid sarcoplasmic overload of Ca^{2+}. Supplemental Fig. 1 shows the morphology of isolated rat CMs, indicating their rectangular shape with a distinct rod-shaped appearance and clear striations. In addition, we cultured the isolated CMs to let them be recovered from the stresses and damage that occurred during the enzymatic digestion and physical disruption of the isolation procedure. We did not note changes in the cell contours of CMs after exposure to agonists such as C5a, but we did not rule out subtle changes, such as membrane ruffling after exposure to C5a. We have shown how these CMs respond to histones (31) or C5a (7), which were not toxic for the cells (no apoptosis or release of LDH).

Permeabilization of CMs and intracellular antibody staining

For assessment of intracellular staining by flow cytometry, CMs were fixed in 0.25% paraformaldehyde at 4°C for 30 min. The cells were permeabilized with 1% saponin (Sigma-Aldrich, St. Louis, MO, USA) at room temperature for 60 min. Incubation with the antibodies was performed in the presence of 0.1% saponin in the dark at room temperature for 30 min. The following conjugated antibodies from BD Biosciences (Franklin Lakes, NJ, USA) were used to evaluate MAPK phosphorylation: BD Phosflow Alexa Fluor 488 mouse anti-ERK-1/2 (p202/pY204); BD Phosflow Alexa Fluor 488 mouse anti-Akt (pS473), clone: M89-61; and BD Phosflow PE mouse anti-p38 MAPK (pT180/pY182). Unconjugated BD Phosflow polyclonal rabbit anti-JNK-1/2 (pT183/pY185) antibody was used in combination with fluorescein (FITC)-conjugated AffiniPure F(ab')$_2$ fragment goat anti-rabbit IgG (H+L) purchased from Jackson ImmunoResearch (West Grove, PA, USA). In Supplemental Fig. 2*A–D* are examples of flow cytometry graphs showing fluorescence-activated cell-sorting profiles for each antibody in rat CMs.

Immunostaining of frozen left ventricular sections for MAPKs

All immunostaining was performed on fresh-frozen 4-μm–thick left ventricular (LV) sections of mouse heart tissue, embedded in optimal cutting temperature compound (Fisher Healthcare, Houston, TX, USA). The following individual or multiple primary antibodies were used: monoclonal anti-troponin-T cardiac isoform Ab-1 (clone 13-11; Lab Vision; Thermo Fisher Scientific, Waltham, MA, USA), rabbit anti-phospho-p44/42 MAPK (ERK-1/2) (Thr202/Tyr204) antibody (Cell Signaling Technology, Danvers, MA, USA), and rabbit anti-phospho-p38 (Thr180/Tyr182) antibody (Cell Signaling Technology). Secondary antibodies were as follows: anti-mouse IgG conjugated to Alexa Fluor 647 and anti-rabbit IgG conjugated to Alexa Fluor 488 (both from Jackson ImmunoResearch Laboratories). The slides were mounted with ProLong Gold antifade reagent containing DAPI (Thermo Fisher Scientific) and viewed with an Axio fluorescence microscope with Axio Vision software (Zeiss, Jena, Germany). Negative staining controls lacking primary antibody were always performed.

Isolating and treating peritoneal exudate macrophages

Mouse peritoneal exudate macrophages (PEMs) were isolated 4 d after the injection of 1.5 ml 2.4% thioglycolate, i.p. (Thermo Fisher Scientific), according to our published procedure (32, 33). PEMs were treated with LPS (100 ng/ml, 1 h at 37°C), with or without p38 inhibitor.

Cytokine and histone ELISAs

Cytokine (IL-6, IL-1β, and TNF) ELISAs were from R&D Systems (Minneapolis, MN, USA) and performed per the manufacturer's recommendations. The histone ELISA (Cell Death Detection

ELISA) was from Roche (Indianapolis, IN, USA). Purified mixed calf thymus histones were used to generate standard curves (34).

Bio-Plex phosphoprotein assay

The Bio-Plex phosphoprotein assay was used to detect the presence of phosphorylated p38, ERK-1/2, JNK-1/1, and Akt in PEMs after the exposure to LPS (100 ng/ml, 1 h at 37°C). The assay kit and the phosphoprotein testing reagent kit (Bio-Rad Laboratories, Hercules, CA, USA) were used according to the manufacturer's protocol.

Reagents

The reagent used in this study, recombinant rat (rr)C5a, was produced by us (8, 35). The chemicals used for preparation of solutions for CM isolation and LPS were purchased from Sigma-Aldrich.

In our first set of experiments, DMSO-soluble inhibitors for MAPKs (p38, JNK-1/2, and ERK-1/2) and Akt were used. Our functional data, obtained with Doppler echocardiography (echo Doppler), from septic mice treated with one of these inhibitors showed the same response as the mice treated with DMSO alone (data not shown), indicating the antioxidant effects of DMSO, *per se*. To avoid any artificial antioxidant properties of the other DMSO-soluble MAPK inhibitors (36), in our second set of experiments we used a water-soluble MAPK inhibitor that, so far, is available only for p38. Water-soluble salt of p38 inhibitor (SB 203580), purchased from Tocris Bioscience (Bristol, United Kingdom), was therefore used in the current study. For *in vivo* experiments, 20 mg/kg, i.p. of the inhibitor was used 2 h before inducing CLP to study the effects of this inhibitor on the activation pattern occurring after sepsis, by measuring histone and cytokines (IL-6 and -1β) levels in the plasma, as well as activation of MAPK and Akt in the heart tissue. For *in vitro* experiments, different doses (5–50 μM) of this inhibitor were used to find the half maximum inhibitory concentration (IC_{50}) for further *in vitro* experiments.

Echocardiography

Echocardiography was performed, according to a published procedure (7, 30, 31), by a registered echocardiographer who was blinded to the treatment groups of mice. Wild-type (WT) C57BL/6 mice were weighed and anesthetized with inhaled isoflurane. Imaging was performed with a Vevo 770 High-Resolution *In Vivo* Imaging System (Visualsonics, Toronto, ON, Canada) equipped with an RMV-707 30-MHz RMV (up to 45 MHz) scan head (real-time visualization). Details of measuring systolic and diastolic parameters by echo Doppler are described in our previous reports (7, 30, 31). Imaging was performed before and 8 h after CLP.

Statistical analysis

Data were expressed as means ± SEM and analyzed with Prism 7 graphing and statistical analysis software (GraphPad, Inc., La Jolla, CA, USA). Significant differences between groups were determined by 1-way ANOVA or Student's *t* test, as appropriate. Significance was set at $P < 0.05$.

RESULTS

C5a-induced activation of Akt and MAPKs in CMs

Rat cardiomyocytes were cultured in PBS buffer (control) or in the presence of recombinant rat (rr)C5a (1 μg/ml) at 37°C for various times (**Fig. 1**). Based on flow cytometry analysis of saponin-permeabilized CMs, phosphorylation of Akt and MAPKs occurred as a function of time of exposure to C5a. We used mAbs that had as targets phosphoserine, phosphothreonine, or phosphotyrosine. In the case of Akt, phosphorylation was clearly evident by 60 min, persisting for up to 120 min, and

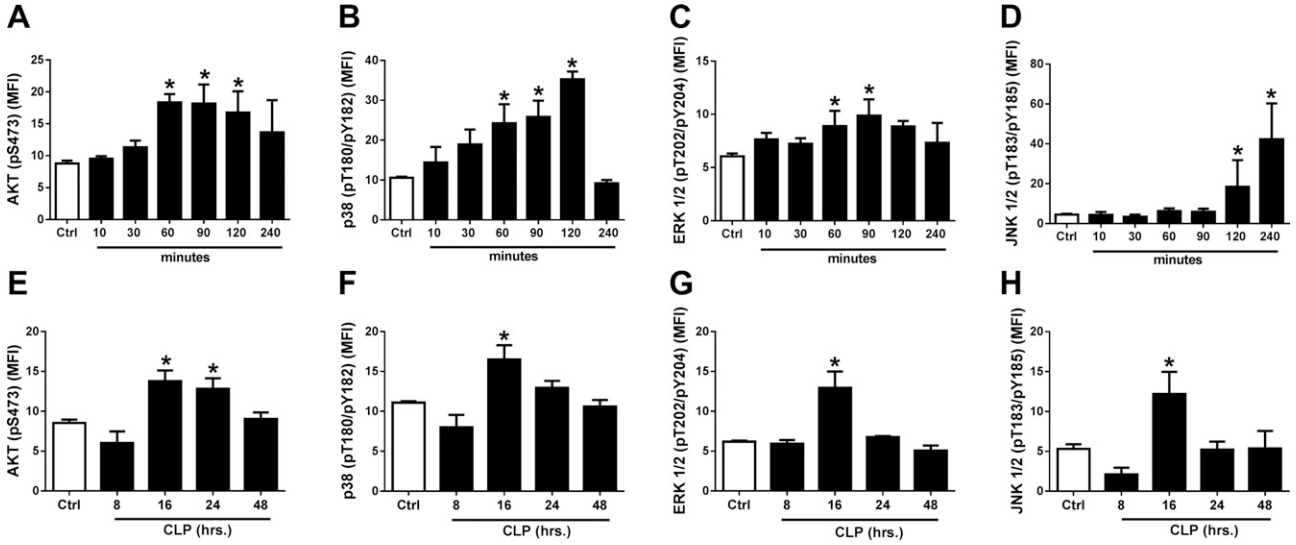

Figure 1. Time courses for C5a-induced (1 μg rrC5a/ml) *in vitro* activation (phosphorylation) of Akt (*A*, *E*) and the 3 MAPKs (p38, *B*, *F*; ERK-1/2, *C*, *G*; and JNK-1/2, *D*, *H*) in rat CMs. Using antibodies to phosphoamino acids in Akt or in MAPKs, end points were determined by flow cytometry in saponin-permeabilized rat CMs. *A–D*) On the vertical axes are the antibody targets (phosphoserine, phosphothreonine, or phosphotyrosine). On the horizontal axes are the time courses (min) of activation. *E–H*) The time courses (h) for CLP-induced activation (phosphorylation) of Akt and MAPKs in permeabilized rat CMs as a function of time after CLP. MFI, mean fluorescence intensity, indicating levels of phospho-MAPK and phospho-Akt. Ctrl, control CMs from sham-treated rats. Data are expressed as means ± SEM ($n \geq 6$ for all time groups). *$P < 0.05$.

thereafter decreasing (Fig. 1*A*). In the case of p38, there was progressive phosphorylation from 60–120 min, followed by rapid decline after 4 h (Fig. 1*B*). In the case of ERK-1/2, phosphorylation peaked at 60 and 90 min, followed by a decline (Fig. 1*C*). Phosphorylation of JNK-1/2 was not found until 120 and 240 min after C5a exposure (Fig. 1*D*). Clearly, CMs exposed *in vitro* to C5a (1 μg/ml) were activated as a function of time of exposure to C5a for all 3 MAPKs, as well as for Akt.

Figure 1*E–H* demonstrates activation in CMs of Akt and all 3 MAPKs as a function of time after CLP (8–48 h). Phosphorylation of Akt peaked at 16 and 24 h after CLP, followed by a decline (Fig. 1*E*). A peak in phosphorylation of p38 occurred 16 h after CLP, followed by a decline (Fig. 1*F*). For activation of ERK-1/2 (Fig. 1*G*), the pattern was similar to that for p38, peaking at 16 h. For JNK-1/2 (Fig. 1*H*), activation after CLP also peaked at 16 h, followed by a decline. Accordingly, CLP caused activation of Akt as well as p38, ERK-1/2, and JNK-1/2 in CMs as a function of time after the onset of sepsis.

CLP-induced activation of Akt and MAPKs in LV CMs and requirement for C5aRs

For these experiments, frozen LV sections of mouse hearts were obtained from WT control mice before and, where indicated, from C5aR-knockout (KO) mice, 16 h after CLP. There was virtually no staining in WT control (sham-treated) hearts, but in WT hearts 16 h after CLP, intense green fluorescence indicated presence of phospho-ERK-1/2, which was greatly diminished in hearts from 16 h CLP mice lacking either C5aR (**Fig. 2*A***, top). The frozen LV sections revealed intense red fluorescence for troponin-T (TnT) and similar patterns of green staining for phospho-ERK-1/2 16 h after CLP (Fig. 2*A*, bottom). Yellow-green fluorescence and blue nuclear (DAPI) stain, indicated a merger of fluorescence-labeled TnT and phospho-ERK-1/2.

CLP was associated with intense green staining for phospho-p38 in LV CMs. In C5aR-KO CLP mice, the fluorescence for activated p38 was barely detectable (Fig. 2*B*, top). There was intense red fluorescence for TnT, green fluorescence for phospho-38, with the merged image showing blue fluorescence for nuclear staining and yellow-green fluorescence (Fig. 2*B*, bottom). CLP induced staining of green fluorescence for phospho-Akt and for phospho-JNK-1/2 (Fig. 2*C*, *D*). In each case, the absence of C5aRs caused reduced evidence for activation of Akt and JNK-1/2 after CLP. Taken together, the data indicate that, after CLP, C5a and its receptors activate Akt and MAPKs in CMs, which may be linked to the development of septic cardiomyopathy.

Reduced plasma histones IL-6 and IL-1β in CLP mice pretreated with water-soluble p38 inhibitor

Eight hours after CLP, 10 CLP WT mice that received 1.0 ml PBS, i.p., and 10 CLP mice treated with the p38 inhibitor (SB203580) were compared for levels of plasma histones and cytokines, which are reliable plasma biomarkers for the intensity of sepsis (31) (**Fig. 3**). The time point of 8 h after CLP was selected, because, at this time point, there is clear dysfunction of hearts based on echo Doppler parameters (7, 30, 31). The mice received the water-soluble p38 inhibitor (20 mg/kg in a volume of 1.0 ml PBS, i.p.), which was injected 2 h before the onset of CLP. The positive reference group received 1.0 ml PBS, i.p. 2 h before CLP. At 8 h after CLP, plasma (using acid-citrate-dextrose as the anticoagulant) was obtained from the inferior vena cava and analyzed by ELISA for histone and cytokine content. Nonmeasurable levels of histones and cytokines were present in plasma before CLP (data not shown). There was a 58% reduction in plasma levels of histones in CLP mice that received the water-soluble p38 inhibitor (Fig. 3*A*), when compared to the CLP group receiving PBS. There was a 38% reduction in the amount of plasma IL-6 (Fig. 3*B*) and a 45% reduction in plasma IL-1β (Fig. 3*C*) in CLP mice pretreated with the water-soluble inhibitor of p38. We have recently shown (31) that reduced plasma histone levels also occurred in CLP mice that lacked either of the two C5aRs or in mice that were devoid of the nucleotide-binding domain and leucine-rich repeat pyrin domain–containing protein-3. In such cases, the KO mice were protected from the full development of cardiac dysfunction after CLP (as demonstrated by echo Doppler parameters) (7), indicating that the sepsis-induced cardiac defects also require participation of nucleotide-binding domain and leucine-rich repeat pyrin domain–containing protein-3 and both C5aRs.

Ability of the p38 inhibitor to suppress *in vitro* activation of MAPKs and Akt in LPS-stimulated PEMs

Mouse PEMs (1×10^6) were exposed to PBS buffer (negative control) or to LPS (100 ng/ml) for 1 h at 37°C, after which cells were assessed by the Bio-Plex phosphoprotein assay for activation of p38, ERK-1/2, JNK-1/2, and Akt, using the antibodies described in Fig. 1. LPS caused activation of Akt and all 3 MAPKs (Fig. 4*A–D*). The most robust activation involved ERK-1/2 (nearly a 13-fold increase). In the absence of detailed studies (LPS dose responses) it is premature to come to definitive conclusions about the rank order of MAPK and Akt activation. LPS activation of PEMs included a 4-fold increase in phospho-p38 (Fig. 4*A*), a 13-fold increase in ERK-1/2 (Fig. 4*B*), and a 7-fold increase in phospho-JNK (Fig. 4*C*), along with a small increase in phospho-Akt (Fig. 4*D*).

Mouse PEMs were activated *in vitro* with LPS (100 ng/ml) for 4 h at 37°C in the presence of (1 h preincubation) increasing amounts (5–50 μM) of the water-soluble p38 inhibitor (Fig. 4*E*, *F*). There was a dose-dependent reduction of IL-6 and -1β in cell supernatant fluids that ranged from 10 to 17 μM of the water-soluble inhibitor, allowing us to calculate the IC_{50} of the p38 inhibitor for use in the flow cytometry experiments (Fig. 4*G–K*).

We used PEMs exposed to buffer (negative control) or to LPS (100 ng/ml) in the absence or presence (1 h preincubation) of the 20 μM water-soluble p38 inhibitor (a dose close to its IC_{50}; Fig. 4*G–K*). Cells were then incubated at 37°C for 1 h with LPS. After LPS treatment, cells were incubated in cytofix/cytoperm solution (BD Cytofix; BD Biosciences)

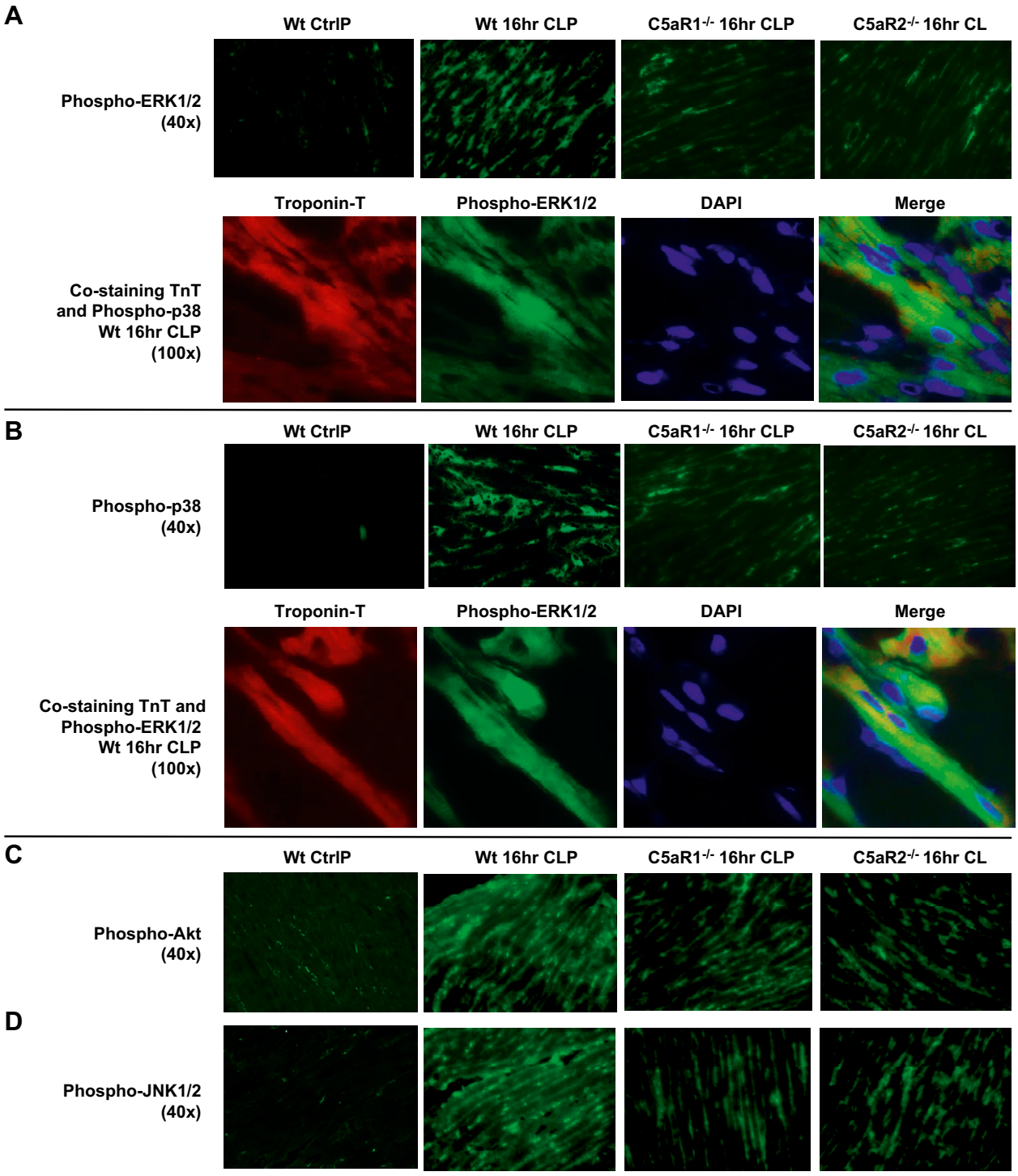

Figure 2. Phospho-MAPKs and Akt before (Ctrl, control) and 16 h after CLP, in frozen LV sections of WT mouse hearts or C5aR-KO mouse hearts. *A*) Phospho-ERK-1/2 before (Ctrl) or 16 h after CLP. Red: TnT; green: phospho-ERK-1/2; blue: DAPI-stained nuclei; yellow-green: merged image of TnT and ERK-1/2 labeling in CMs. *A*) Top: phospo-ERK-1/2 revealed green staining of CMs 16 h after CLP. The staining was markedly reduced in CLP CMs from C5aR-KO mice. *B*) Phospho-p38 images were very similar to those for phospho-ERK-1/2. *C*, *D*) Phospho-Akt (*C*) and phospho-JNK-1/2 (*D*) 16 h after CLP in WT CMs and CMs with and without C5aR1 and -R2. There were marked reductions in phospho-Akt and phospho-JNK-1/2 in frozen LV sections from C5aR-KO mice ($n \geq 3$ for each group of frozen sections).

for 20 min and permeabilized with Perm Buffer III (BD Biosciences) for intracellular staining. Stained cells with BD Phosflow MAPK and Akt antibodies were fixed with 2% paraformaldehyde and evaluated for phosphoproteins by flow cytometry, as described elsewhere (37, 38). Typical traces produced by flow cytometry included buffer-treated cells (negative control), LPS-treated cells, and cells exposed to both LPS and the water-soluble p38 inhibitor (20 μM). Activation of p38 was clearly visible by the shift to the right of cells exposed to LPS (Fig. 4*G*). It was also clear that

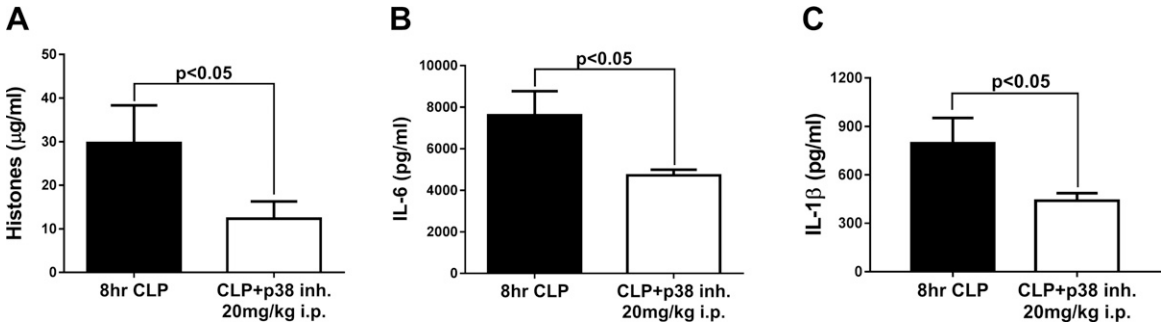

Figure 3. Treatment of CLP mice with a water-soluble p38 inhibitor, which was given 2 h before CLP. As measured by ELISA, there were sharp reductions 8 h after CLP in plasma biomarkers of sepsis: extracellular histones (*A*), IL-6 (*B*), and IL-1β (*C*) (n = 10 mice per marker). Data are expressed as means ± SEM.

the inhibitor interfered with the rightward shift. Activation of the p38 inhibitor was reduced in activation (phosphorylation) of MAPKs and Akt in PEMs, with reductions varying from 46 to 64% (Fig. 4*H–K*). Taken together, the evidence showed that the water-soluble inhibitor p38 also suppressed activation of all 3 MAPKs and Akt in PEMs exposed to LPS.

Ability of water-soluble inhibitor p38 to reduce activation of MAPKs in LV CMs 16 h after CLP and reduction of cytokine release from LPS-stimulated PEMs

Using protocols similar to those in Fig. 2, the immunofluorescence images in **Fig. 5** indicate that LV CMs 16 h after CLP demonstrated activation of MAPKs (Fig. 5*A*, *C*, *E*) and Akt (Fig. 5*G*), whereas LV CMs in mice treated with the water-soluble p38 inhibitor showed very little evidence of kinase activation after CLP (Fig. 5*B*, *D*, *F*, *H*), although nuclear staining with DAPI was evident. These data are consistent with those in Fig. 3, in which mice 8 h after CLP showed reduced plasma levels of extracellular histones IL-6 and -1β. When combined, the data in Fig. 5 indicate that the water-soluble p38 inhibitor inhibits activation of all 3 MAPKs as well as Akt in mice that undergo CLP.

The p38 inhibitor preserves cardiac performance after CLP

As has been reported, CLP induces numerous defects in echo Doppler parameters of cardiac performance (7, 30). In **Fig. 6**, 8 h after CLP, there was a significant reduction in heart rate, LV stroke volume, and cardiac output and an increase in ejection fraction (Fig. 6*A–D*). In mice injected intraperitoneally with the p38 inhibitor 2 h before CLP, there was modest improvement in systolic performance. Mice receiving the p38 inhibitor had a reduction in LV stroke volume and an increased ejection fraction after CLP that was similar to that noted in control mice (Fig. 6*B*, *D*). Injection of the p38 inhibitor resulted in attenuation of the decline in cardiac output after CLP, but there was no significant difference in the post-CLP cardiac output of animals that did or did not receive the p38 inhibitor (Fig. 6*C*). The preservation of heart rate after CLP by p38 inhibition reached clinical significance (Fig. 6*A*). Like cardiac systolic function, cardiac diastolic function was impaired 8 h after induction of CLP. Isovolumic relaxation time (IVRT) and mitral valve (MV) deceleration time were prolonged, and the E-wave (early)/A-wave (late) diastolic filling velocity (E/A) ratio was reduced, suggesting impaired diastolic function 8 h after CLP (Fig. 6*E, G, H*). Injection of a p38 inhibitor before CLP resulted in preservation of diastolic performance: IVRT 17.4 ms (p38 control) *vs.* 17.8 ms (p38 injected) (Fig. 6*E*); E/A ratio: 1.4 (p38 control) *vs.* 1.2 (p38 injected) (Fig. 6*G*); and MV deceleration time: 11.7 ms (p38 control) *vs.* 11.2 ms (p38 injected) (Fig. 6*H*). These data suggest that the water-soluble inhibitor of p38 greatly suppressed sepsis-induced development of cardiac dysfunction. Unfortunately, the lack of commercially available p38-KO mice prevented experiments that would have definitively determined the effects of its absence on development of cardiac dysfunction after sepsis.

DISCUSSION

In the current report, we showed C5a-dependent activation (phosphorylation) of MAPKs and Akt in mouse heart after polymicrobial sepsis. In our earlier studies, we found evidence of involvement of Akt or MAPKs signaling in the heart and phagocytes in CLP-induced sepsis (11, 39, 40). Our data have suggested that the PI3-K/Akt signaling pathway controls various C5a-mediated effects on neutrophil and monocyte innate immunity during experimental sepsis (39). We have shown the ability of C5a to cause activation of ERK-1/2 and p38 MAPK signaling pathways on neutrophils during sepsis in a C5a/C5aR-dependent manner (40). In the current study, we expand our data to investigate activation of MAPKs (p38, ERK-1/2, and JNK-1/2) and Akt in the CMs from CLP mice or after *in vitro* exposure to C5a.

After *in vitro* exposure of CMs to C5a, it was clear that there was activation (phosphorylation) of MAPKs (p38, ERK-1/2, and JNK-1/2) as well as Akt (Fig. 1*A–D*). These responses were both time-dependent and C5a concentration dependent. These data suggest that C5a plays a role in MAPK and Akt signaling pathways in CMs. Furthermore, flow cytometric analysis of CMs revealed activation of MAPKs and Akt in LV CMs as a function of time after onset of CLP (Fig. 1*E–H*), suggesting the activation of MAPK and Akt signaling pathways after CLP in CMs.

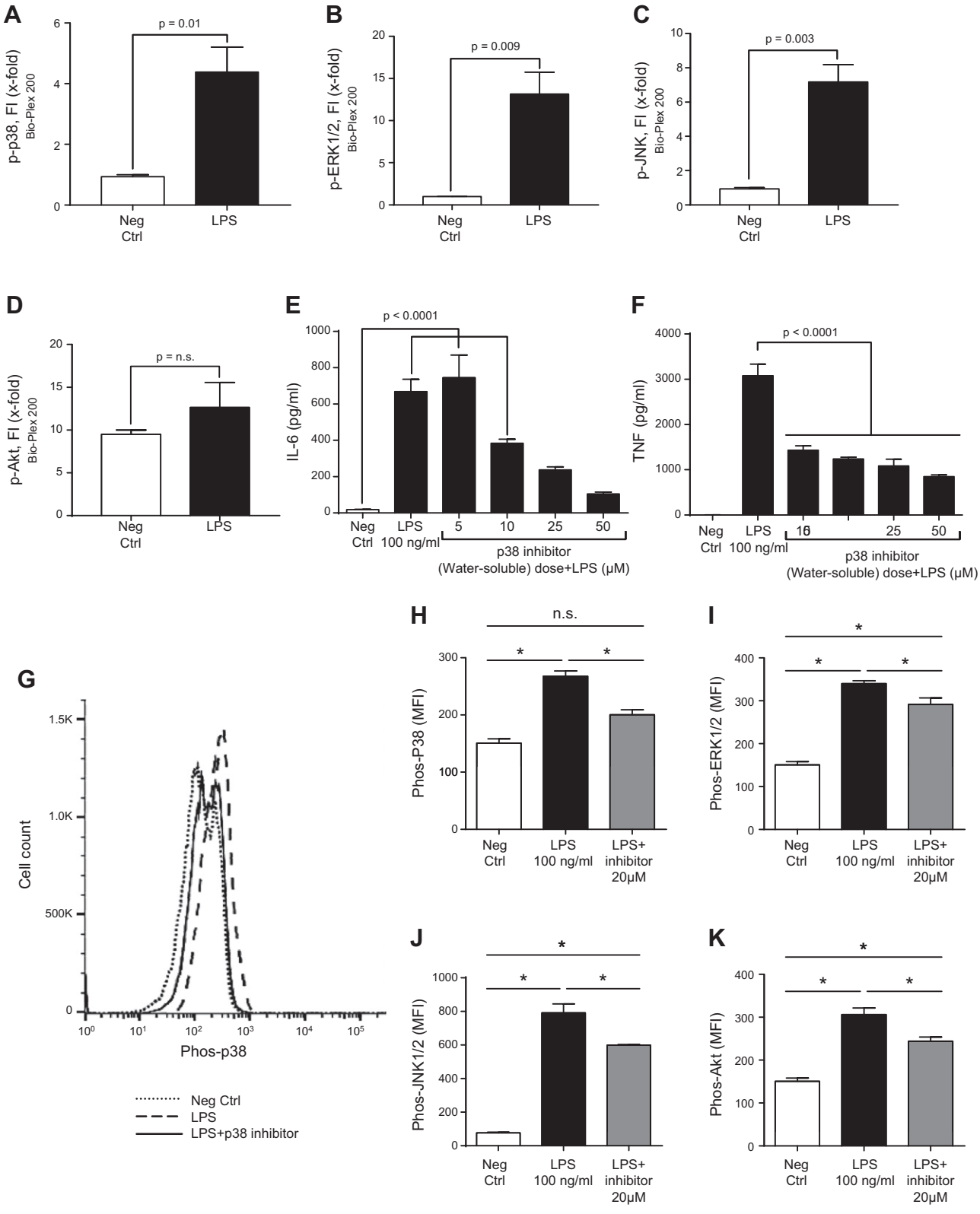

Figure 4. Phosphorylation of mouse PEMs (1 h at 37°C) caused by LPS (100 ng/ml). *A–D*) Bio-Plex phosphoprotein assay analysis of intracellular phospho-MAPKs p-p38 (*A*), p-ERK1/2 (*B*), and p-JNK (*C*) or p-AKT (*D*). Neg Ctrl, negative control. *E*, *F*) Dose response test of water-soluble p38 inhibitor (5–50 μM), in which the IC_{50} was used, indicated a dose-related reduction in release of IL-6 (*E*) and TNF (*F*). *G–K*) *In vitro* reductions in phospho-MAPKs and Akt in PEMs exposed to LPS in the absence or presence of 20 μM water-soluble inhibitor of p38. *G*) Typical example of PEMs exposed to buffer (neg ctrl) or to LPS in the presence or absence of the p38 inhibitor, using flow cytometry as the end point for phospho-Akt or phospho-MAPKs, as described in Fig. 1. *H–K*) Levels of mean fluorescence intensity (MFI) indicating the levels of phospho-MAPKs p-p38 (*H*), p-ERK1/2 (*I*), and p-JNK (*J*) or p-AKT (*K*) in PEMs exposed to LPS in the absence or presence of 20 μM water-soluble inhibitor of p38. Data are expressed as means ± SEM ($n \geq 5$ samples per group). $^*P < 0.05$.

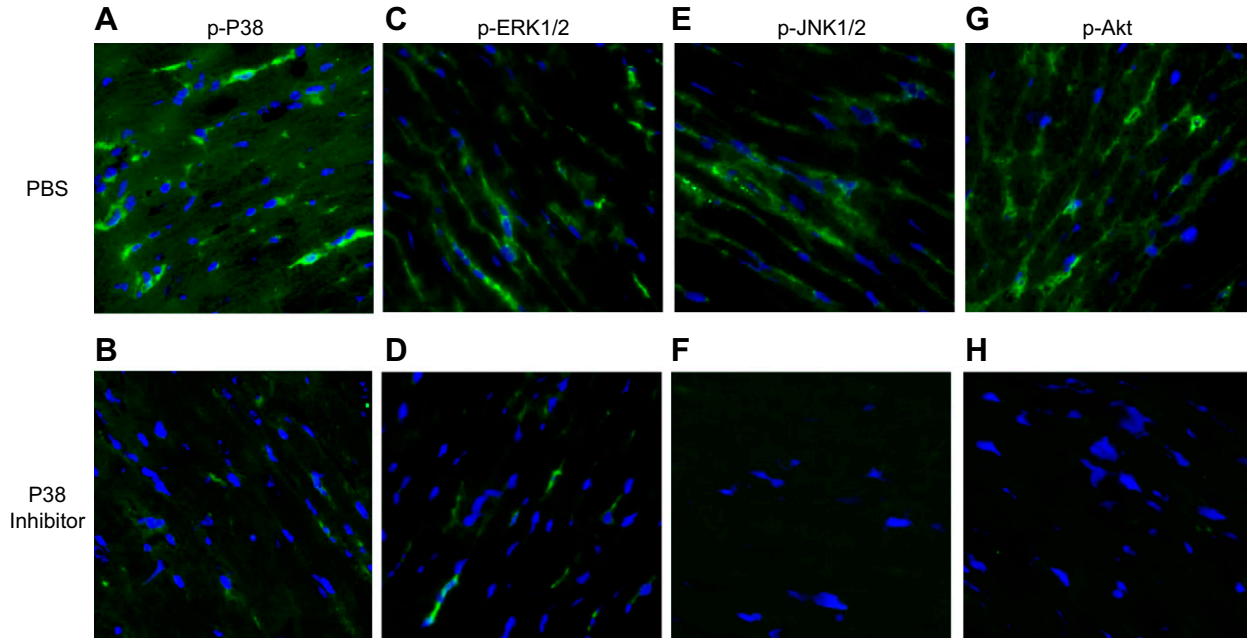

Figure 5. Blockage of activation of MAPKs by water-soluble p38 inhibitor 16 h after CLP, determined with techniques similar to those described in Fig. 2. *A*, *C*, *E*, *G*) At 16 h after CLP, CMs demonstrated phosphorylation of MAPKs p38 (*A*), ERK1/2 (*C*), and p-JNK (*E*) and AKT (*G*). Green: MAPK; blue: DAPI. *B*, *D*, *F*, *H*) Pre-CLP administration of the p38 inhibitor blocked activation in CMs of all 3 MAPKs (p38, *B*; ERK1/2, *D*; and p-JNK, *F*) and AKT (*H*). (n = 4 separate samples in each group).

Our immunofluorescent analysis of frozen LV sections of WT mouse hearts confirmed these findings, as it showed the activation of MAPKs and Akt in CMs after CLP. Hearts from mice genetically deficient in either C5aR-1 or -2 revealed that activation of MAPKs and Akt in CMs required availability of both C5aRs (Fig. 2). These data suggest that the activation of MAPKs and Akt in a septic heart is C5aR dependent. These findings are in line with the previous reports of neutrophils or macrophages stimulated with C5a or LPS (41–43).

Our immunofluorescence staining showed localization of activated Akt and JNK-1/2 (Fig. 2*C*, *D*) in both cytoplasm and nucleus, but in the case of p38 and ERK-1/2 the staining was only cytosolic and not nuclear (Fig. 2*A*, *B*). We did not study any specific isoform of p38, but the literature reported that localization of p38 is likely to be isoform specific. For

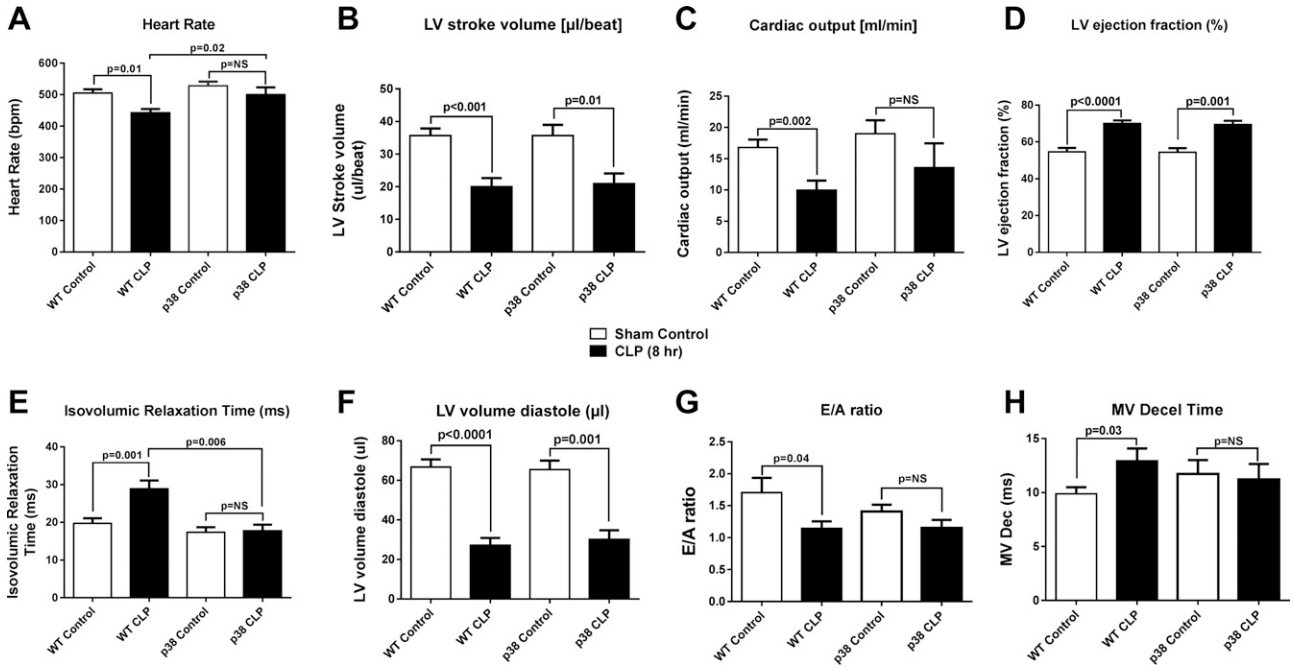

Figure 6. Echo Doppler parameters in hearts of mice before (WT control) and 8 h after CLP. Heart rate (*A*), LV stroke volume (*B*), cardiac output (*C*), LV ejection fraction (*D*), IVRT (*E*), LV volume diastole (*F*), E/A ratio (*G*), and MV deceleration time (*H*). Data are expressed as means ± SEM ($n \geq 6$ mice per group).

example, the p38-α MAPK has been identified as a nuclear protein in its inactive state, bound to its substrate MAPKAPK-2 (MAPK-activated protein kinase-2). After activation, p38-α MAPK phosphorylates MAPKAPK-2, and this phosphorylation masks a nuclear localization signal in MAPKAPK-2, resulting in the export of both proteins to the cytoplasm (44). Court *et al.* (45) showed both cytosolic and nuclear localization of p38 family members on CMs. They showed nonnuclear localization of p38-γ (stress-activated protein kinase-3) staining on rat and mouse heart. In fact, inactive p38-γ is cytoplasmic compared to the nuclear localization of inactive p38-α/β (44, 45). The localization of ERK-1/2 can be dependent on the intensity of the activation (phosphorylation). Rubinfeld *et al.* (46) showed that overexpression of ERK-1/2 in cells frequently drives them into the nucleus, presumably by overwhelming cytosolic binding sites. They showed that coexpression of the ERK-2 with its upstream activator, MEK-1, results in cytosolic retention of the ERK-2, which is the result of its association with MEK-1 and is reversed upon stimulation (46). In earlier report, Zheng *et al.* (47) showed that ERK is phosphorylated and activated in the cytoplasm, and the activated ERK could subsequently translocate into the nucleus and phosphorylate its nuclear substrates. They showed MEK (MAPK or ERK) is localized exclusively in the cytoplasm, as measured by indirect immunofluorescence, subcellular fractionation, and detergent permeabilization techniques. In contrast to ERK, MEK was not translocated into the nucleus when cells were treated with mitogens, indicating that ERK is phosphorylated and activated by MEK in the cytoplasm (47). They compared their immunofluorescence findings with other reports, of which some showed that both cytoplasm and nucleus localization of ERK depends on the cell types.

Most of the studies on MAPK signaling pathways are descriptive, and it is difficult to determine how the signaling pathways between individual MAPKs and their interactions work. One of the ways to study MAPK signaling pathways is using MAPK inhibitors. In Fig. 3, we used the p38 inhibitor to see whether its blocking can reduce the adverse outcome after sepsis as p38 MAPK is suggested to be a key signaling molecule in septic lung injury (48) and has been shown to be a therapeutic target in inflammatory diseases (14). There are also substantial data in mice, showing that inhibition of p38 MAPK may have protective effects against development of cardiac hypertrophy and dysfunction (49), as well as in other diseases such as acute liver failure (50) and arthritis (51). Our studies involved systemic administration of a water-soluble p38 inhibitor, avoiding the difficulties of artifacts induced by MAPK inhibitors that require solubilization of inhibitors in DMSO, which has strong antioxidant effects (36). Administration of the water-soluble inhibitor of p38 caused reductions in 3 plasma products after CLP: extracellular histones, IL-6, and IL-1β, which are known to be quantitatively linked to the intensity of the sepsis and its progression (29–31). In CLP WT mice treated with the p38 inhibitor, there were substantial reductions in plasma histones and proinflammatory cytokines (Fig. 3), as well as reduced evidence of CLP-induced abnormalities in echo Doppler parameters (Fig. 6).

In our earlier reports, we showed a relationship between plasma histones and cardiac dysfunction (31), in which histones caused dysfunction in hearts after polymicrobial sepsis and also when hearts were perfused with histones, leading to electrical and functional dysfunction. Such abnormalities could be prevented by infusion of a neutralizing mAb to histone. We also showed that *in vivo* neutralization of histones in septic mice markedly reduced the parameters of heart dysfunction, as measured by echo Doppler techniques (31). In the current study, we showed treatment of CLP mice with the water-soluble p38 inhibitor reduced echo Doppler abnormalities in the heart developing after CLP (Fig. 6) and diminished the evidence for activation of MAPKs and Akt in LV CMs (Fig. 5). It was also obvious that the inhibitor decreased LPS-induced activation of MAPKs and Akt in PEMs stimulated with LPS (Fig. 4).

However, at this point, the story becomes somewhat confusing, because the use of the p38 inhibitor not only suppressed activation of p38 (as determined by immunostaining of frozen LV sections from WT CLP hearts for activated p38), but also reduced activation of Akt, ERK-1/2, and JNK-1/2 in LV CMs (Fig. 5). We were also able to show *in vitro* that incubation of peritoneal macrophages with LPS, which is a potent microbial mediator and is sometimes implicated in the pathogenesis of sepsis, resulted in activation of Akt and all 3 MAPKs and that the *in vitro* presence of the water-soluble p38 inhibitor reduced activation of all 4 signaling molecules with IC_{50}s between 10 μM (TNF) and 17 μM (IL-6) (Fig. 4). There are two possible explanations for these findings: the water-soluble p38 inhibitor has broad inhibitor activities for MAPKs that extend beyond p38; or alternatively, it is possible that p38 is the first in a sequence of activation events of signaling molecules (ERK-1/2, JNK-1/2, and Akt), such that blockade of p38 blocks these downstream activation events. It is difficult at present to select which early explanation is more likely.

Therapeutic approaches for treatment of septic cardiomyopathy have been under intensive investigation in recent years. In the past decade, strategic targets were cardiosuppressive activities in cytokines, such as TNF (52), or suppression of signaling pathways leading to NF-κB activation (53). The multiplicity of cytokines capable of ultimately causing cardiac or CM dysfunction suggests that a therapeutic focus on blockade of a single cytokine probably will not be therapeutically effective. In support of these reservations, clinical trials in septic patients in general failed to convincingly demonstrate a beneficial outcome with TNF or TNF-R blocking agents (54, 55). However, MAPK signaling may be a promising therapeutic target in the setting of septic cardiomyopathy. Based on information in this report, candidates for therapeutic blockade developing in septic cardiomyopathy could be p38. Compounds blocking p38 have been developed for use in Alzheimer's disease (56), but without convincing efficacy, whereas drugs such as vemurafenib (which inhibits phosphorylation of ERK-1/2) have not been successful in Alzheimer's disease, but they have not been evaluated in sepsis. Currently, phase II clinical trials with vemurafenib are under way in patients with metastatic melanoma (57). In the heart, inhibition of MAPK

signal pathways have shown encouraging results in the case of dilated cardiomyopathy (58), but it is too early to speculate whether such interventions would be useful for treatment of sepsis-induced cardiomyopathy.

CONCLUSIONS

In the setting of polymicrobial sepsis in mice, complement activation develops and is linked to the development of septic cardiomyopathy. In the current study, we showed that the complement anaphylatoxin C5a reacts with its receptors on CMs. This *in vitro* incubation of CMs causes activation of MAPKs and Akt. Furthermore, isolation of CMs demonstrated phosphorylation of MAPKs (p38, ERK-1/2, and JNK-1/2) and Akt after sepsis, all of which was C5aR dependent. These data together suggest the role of C5a in activating MAPK and Akt signaling pathways and the development of cardiac dysfunction after polymicrobial sepsis. *In vivo* use of a water-soluble inhibitor of p38 blocked activation in CMs of MAPKs and Akt in septic mice. This resulted in protection of CMs from developing the full expression of defective echo Doppler parameters after the onset of sepsis. FJ

ACKNOWLEDGMENTS

The authors thank the Microscopy and Image Analysis Laboratory (MIL), University of Michigan (UM) Medical School, a multiuser imaging facility supported by a grant from the U.S. National Institutes of Health (NIH) National Cancer Institute; the O'Brien Renal Center, the UM Medical School, the Endowment for the Basic Sciences (EBS), and the UM Department of Cell and Developmental Biology; Kimber Converso-Baran, research sonographer and echocardiographic specialist, for excellent services provided; and Sue Scott, Melissa Rennells, and Michelle Possley (all from UM) for excellent assistance in the preparation of the manuscript. This study was supported by NIH, General Medicine Grants GM-29507 and GM-61656 (to P.A.W.), the Deutsche Forschungsgemeinschaft Fellowship Project KA 3740 (to M.K.); Deutsche Forschungsgemeinschaft Grant BO 3482/3-1 (to M.B.), Federal Ministry of Education and Research Grant 01EO1003 (to M.B.) and HU823/302 (to M.S.H.-L.). F.F. and M.K. are cofirst authors. The authors declare no conflicts of interest.

AUTHOR CONTRIBUTIONS

F. Fattahi, M. Kalbitz, E. A. Malan, E. Abe, L. Jajou, and M. Bosmann performed the experiments, including isolated CMs, flow cytometric and microscopic analyses, and ELISAs; M. W. Russell provided interpretations of echocardiographic data; F. Fattahi, P. A. Ward, and M. Kalbitz wrote the paper; F. S. Zetoune induced experimental sepsis (CLP) in the mice and rats; and M. S. Huber-Lang and P. A. Ward contributed to experimental design and data analysis, coordinated the study, and supervised financial support.

REFERENCES

1. Romero-Bermejo, F. J., Ruiz-Bailen, M., Gil-Cebrian, J., and Huertos-Ranchal, M. J. (2011) Sepsis-induced cardiomyopathy. *Curr. Cardiol. Rev.* **7**, 163–183
2. Fernandes, C. J., Jr., Akamine, N., and Knobel, E. (1999) Cardiac troponin: a new serum marker of myocardial injury in sepsis. *Intensive Care Med.* **25**, 1165–1168
3. Blanco, J., Muriel-Bombín, A., Sagredo, V., Taboada, F., Gandía, F., Tamayo, L., Collado, J., García-Labattut, A., Carriedo, D., Valledor, M., De Frutos, M., López, M. J., Caballero, A., Guerra, J., Alvarez, B., Mayo, A., and Villar, J.; Grupo de Estudios y Análisis en Cuidados Intensivos. (2008) Incidence, organ dysfunction and mortality in severe sepsis: a Spanish multicentre study. *Crit. Care* **12**, R158
4. Ward, P. A., Guo, R. F., and Riedemann, N. C. (2012) Manipulation of the complement system for benefit in sepsis. *Crit. Care Res. Pract.* **2012**, 427607
5. Nakae, H., Endo, S., Inada, K., Takakuwa, T., Kasai, T., and Yoshida, M. (1994) Serum complement levels and severity of sepsis. *Res. Commun. Chem. Pathol. Pharmacol.* **84**, 189–195
6. Huber-Lang, M. S., Sarma, J. V., McGuire, S. R., Lu, K. T., Guo, R. F., Padgaonkar, V. A., Younkin, E. M., Laudes, I. J., Riedemann, N. C., Younger, J. G., and Ward, P. A. (2001) Protective effects of anti-C5a peptide antibodies in experimental sepsis. *FASEB J.* **15**, 568–570
7. Kalbitz, M., Fattahi, F., Herron, T. J., Grailer, J. J., Jajou, L., Lu, H., Huber-Lang, M., Zetoune, F. S., Sarma, J. V., Day, S. M., Russell, M. W., Jalife, J., and Ward, P. A. (2016) Complement destabilizes cardiomyocyte function in vivo after polymicrobial sepsis and in vitro. *J. Immunol.* **197**, 2353–2361
8. Niederbichler, A. D., Hoesel, L. M., Westfall, M. V., Gao, H., Ipaktchi, K. R., Sun, L., Zetoune, F. S., Su, G. L., Arbabi, S., Sarma, J. V., Wang, S. C., Hemmila, M. R., and Ward, P. A. (2006) An essential role for complement C5a in the pathogenesis of septic cardiac dysfunction. *J. Exp. Med.* **203**, 53–61
9. Fattahi, F., and Ward, P. A. (2017) Complement and sepsis-induced heart dysfunction. *Mol. Immunol.* **84**, 57–64
10. Sarma, J. V., and Ward, P. A. (2012) New developments in C5a receptor signaling. *Cell Health Cytoskelet.* **4**, 73–82
11. Zetoune, F. S., Hoesel, L. M., Neiderbichler, A. D., Flierl, M. A., Rittirsch, D., Nadeau, B. A., Sarma, J. V., and Ward, P. A. (2007) Mitogen-activated protein kinases and septic cardiomyopathy. Meeting abstract supplement A1150. *FASEB J.* **21**, 871
12. Johnson, G. L., and Lapadat, R. (2002) Mitogen-activated protein kinase pathways mediated by ERK, JNK, and p38 protein kinases. *Science* **298**, 1911–1912
13. Liu, X., Zhang, C. S., Lu, C., Lin, S. C., Wu, J. W., and Wang, Z. X. (2016) A conserved motif in JNK/p38-specific MAPK phosphatases as a determinant for JNK1 recognition and inactivation. *Nat. Commun.* **7**, 10879
14. Kumar, S., Boehm, J., and Lee, J. C. (2003) p38 MAP kinases: key signalling molecules as therapeutic targets for inflammatory diseases. *Nat. Rev. Drug Discov.* **2**, 717–726
15. Armstrong, S. C. (2004) Protein kinase activation and myocardial ischemia/reperfusion injury. *Cardiovasc. Res.* **61**, 427–436
16. Liu, Y., Shepherd, E. G., and Nelin, L. D. (2007) MAPK phosphatases–regulating the immune response. *Nat. Rev. Immunol.* **7**, 202–212
17. Mockridge, J. W., Marber, M. S., and Heads, R. J. (2000) Activation of Akt during simulated ischemia/reperfusion in cardiac myocytes. *Biochem. Biophys. Res. Commun.* **270**, 947–952
18. Cook, S. A., Sugden, P. H., and Clerk, A. (1999) Activation of c-Jun N-terminal kinases and p38-mitogen-activated protein kinases in human heart failure secondary to ischaemic heart disease. *J. Mol. Cell. Cardiol.* **31**, 1429–1434
19. Haynes, M. P., Li, L., Sinha, D., Russell, K. S., Hisamoto, K., Baron, R., Collinge, M., Sessa, W. C., and Bender, J. R. (2003) Src kinase mediates phosphatidylinositol 3-kinase/Akt-dependent rapid endothelial nitric-oxide synthase activation by estrogen. *J. Biol. Chem.* **278**, 2118–2123
20. Toledo-Pereyra, L. H., Lopez-Neblina, F., Reuben, J. S., Toledo, A. H., and Ward, P. A. (2004) Selectin inhibition modulates Akt/MAPK signaling and chemokine expression after liver ischemia-reperfusion. *J. Invest. Surg.* **17**, 303–313
21. Chen, Y., Ba, L., Huang, W., Liu, Y., Pan, H., Mingyao, E., Shi, P., Wang, Y., Li, S., Qi, H., Sun, H., and Cao, Y. (2017) Role of carvacrol in cardioprotection against myocardial ischemia/reperfusion injury in rats through activation of MAPK/ERK and Akt/eNOS signaling pathways. *Eur. J. Pharmacol.* **796**, 90–100
22. Song, L., Yang, H., Wang, H. X., Tian, C., Liu, Y., Zeng, X. J., Gao, E., Kang, Y. M., Du, J., and Li, H. H. (2014) Inhibition of 12/15 lipoxygenase by baicalein reduces myocardial ischemia/reperfusion injury via modulation of multiple signaling pathways. *Apoptosis* **19**, 567–580
23. Kato, K., Yin, H., Agata, J., Yoshida, H., Chao, L., and Chao, J. (2003) Adrenomedullin gene delivery attenuates myocardial infarction and apoptosis after ischemia and reperfusion. *Am. J. Physiol. Heart Circ. Physiol.* **285**, H1506–H1514

24. Sun, L., Chen, C., Jiang, B., Li, Y., Deng, Q., Sun, M., An, X., Yang, X., Yang, Y., Zhang, R., Lu, Y., Zhu, D. S., Huo, Y., Feng, G. S., Zhang, Y., and Luo, J. (2014) Grb2-associated binder 1 is essential for cardioprotection against ischemia/reperfusion injury. *Basic Res. Cardiol.* **109**, 420
25. Lim, N. R., Thomas, C. J., Silva, L. S., Yeap, Y. Y., Yap, S., Bell, J. R., Delbridge, L. M., Bogoyevitch, M. A., Woodman, O. L., Williams, S. J., May, C. N., and Ng, D. C. (2013) Cardioprotective 3′,4′-dihydroxyflavonol attenuation of JNK and p38(MAPK) signalling involves CaMKII inhibition. *Biochem. J.* **456**, 149–161
26. Du, J., Zhang, L., Wang, Z., Yano, N., Zhao, Y. T., Wei, L., Dubielecka-Szczerba, P., Liu, P. Y., Zhuang, S., Qin, G., and Zhao, T. C. (2016) Exendin-4 induces myocardial protection through MKK3 and Akt-1 in infarcted hearts. *Am. J. Physiol. Cell Physiol.* **310**, C270–C283
27. Höpken, U. E., Lu, B., Gerard, N. P., and Gerard, C. (1996) The C5a chemoattractant receptor mediates mucosal defence to infection. *Nature* **383**, 86–89
28. Gerard, N. P., Lu, B., Liu, P., Craig, S., Fujiwara, Y., Okinaga, S., and Gerard, C. (2005) An anti-inflammatory function for the complement anaphylatoxin C5a-binding protein, C5L2. *J. Biol. Chem.* **280**, 39677–39680
29. Rittirsch, D., Huber-Lang, M. S., Flierl, M. A., and Ward, P. A. (2009) Immunodesign of experimental sepsis by cecal ligation and puncture. *Nat. Protoc.* **4**, 31–36
30. Kalbitz, M., Fattahi, F., Grailer, J. J., Jajou, L., Malan, E. A., Zetoune, F. S., Huber-Lang, M., Russell, M. W., and Ward, P. A. (2016) Complement-induced activation of the cardiac NLRP3 inflammasome in sepsis. *FASEB J.* **30**, 3997–4006
31. Kalbitz, M., Grailer, J. J., Fattahi, F., Jajou, L., Herron, T. J., Campbell, K. F., Zetoune, F. S., Bosmann, M., Sarma, J. V., Huber-Lang, M., Gebhard, F., Loaiza, R., Valdivia, H. H., Jalife, J., Russell, M. W., and Ward, P. A. (2015) Role of extracellular histones in the cardiomyopathy of sepsis. *FASEB J.* **29**, 2185–2193
32. Grailer, J. J., Canning, B. A., Kalbitz, M., Haggadone, M. D., Dhond, R. M., Andjelkovic, A. V., Zetoune, F. S., and Ward, P. A. (2014) Critical role for the NLRP3 inflammasome during acute lung injury. *J. Immunol.* **192**, 5974–5983
33. Fattahi, F., Grailer, J. J., Lu, H., Dick, R. S., Parlett, M., Zetoune, F. S., Nuñez, G., and Ward, P. A. (2017) Selective biological responses of phagocytes and lungs to purified histones. *J. Innate Immun.* **9**, 300–317
34. Bosmann, M., Grailer, J. J., Ruemmler, R., Russkamp, N. F., Zetoune, F. S., Sarma, J. V., Standiford, T. J., and Ward, P. A. (2013) Extracellular histones are essential effectors of C5aR- and C5L2-mediated tissue damage and inflammation in acute lung injury. *FASEB J.* **27**, 5010–5021
35. Huber-Lang, M., Sarma, V. J., Lu, K. T., McGuire, S. R., Padgaonkar, V. A., Guo, R. F., Younkin, E. M., Kunkel, R. G., Ding, J., Erickson, R., Curnutte, J. T., and Ward, P. A. (2001) Role of C5a in multiorgan failure during sepsis. *J. Immunol.* **166**, 1193–1199
36. Bell, J. R., Eaton, P., and Shattock, M. J. (2008) Role of p38-mitogen-activated protein kinase in ischaemic preconditioning in rat heart. *Clin. Exp. Pharmacol. Physiol.* **35**, 126–134
37. Bosmann, M., Patel, V. R., Russkamp, N. F., Pache, F., Zetoune, F. S., Sarma, J. V., and Ward, P. A. (2011) MyD88-dependent production of IL-17F is modulated by the anaphylatoxin C5a via the Akt signaling pathway. *FASEB J.* **25**, 4222–4232
38. Bosmann, M., Sarma, J. V., Atefi, G., Zetoune, F. S., and Ward, P. A. (2012) Evidence for anti-inflammatory effects of C5a on the innate IL-17A/IL-23 axis. *FASEB J.* **26**, 1640–1651
39. Wrann, C. D., Tabriz, N. A., Barkhausen, T., Klos, A., van Griensven, M., Pape, H. C., Kendoff, D. O., Guo, R., Ward, P. A., Krettek, C., and Riedemann, N. C. (2007) The phosphatidylinositol 3-kinase signaling pathway exerts protective effects during sepsis by controlling C5a-mediated activation of innate immune functions. *J. Immunol.* **178**, 5940–5948
40. Riedemann, N. C., Guo, R. F., Hollmann, T. J., Gao, H., Neff, T. A., Reuben, J. S., Speyer, C. L., Sarma, J. V., Wetsel, R. A., Zetoune, F. S., and Ward, P. A. (2004) Regulatory role of C5a in LPS-induced IL-6 production by neutrophils during sepsis. *FASEB J.* **18**, 370–372
41. Chen, N. J., Mirtsos, C., Suh, D., Lu, Y. C., Lin, W. J., McKerlie, C., Lee, T., Baribault, H., Tian, H., and Yeh, W. C. (2007) C5L2 is critical for the biological activities of the anaphylatoxins C5a and C3a. *Nature* **446**, 203–207
42. Hsu, W. C., Yang, F. C., Lin, C. H., Hsieh, S. L., and Chen, N. J. (2014) C5L2 is required for C5a-triggered receptor internalization and ERK signaling. *Cell. Signal.* **26**, 1409–1419
43. Rittirsch, D., Flierl, M. A., Nadeau, B. A., Day, D. E., Huber-Lang, M., Mackay, C. R., Zetoune, F. S., Gerard, N. P., Cianflone, K., Köhl, J., Gerard, C., Sarma, J. V., and Ward, P. A. (2008) Functional roles for C5a receptors in sepsis. *Nat. Med.* **14**, 551–557
44. Ben-Levy, R., Hooper, S., Wilson, R., Paterson, H. F., and Marshall, C. J. (1998) Nuclear export of the stress-activated protein kinase p38 mediated by its substrate MAPKAP kinase-2. *Curr. Biol.* **8**, 1049–1057
45. Court, N. W., dos Remedios, C. G., Cordell, J., and Bogoyevitch, M. A. (2002) Cardiac expression and subcellular localization of the p38 mitogen-activated protein kinase member, stress-activated protein kinase-3 (SAPK3). *J. Mol. Cell. Cardiol.* **34**, 413–426
46. Rubinfeld, H., Hanoch, T., and Seger, R. (1999) Identification of a cytoplasmic-retention sequence in ERK2. *J. Biol. Chem.* **274**, 30349–30352
47. Zheng, C. F., and Guan, K. L. (1994) Cytoplasmic localization of the mitogen-activated protein kinase activator MEK. *J. Biol. Chem.* **269**, 19947–19952
48. Asaduzzaman, M., Wang, Y., and Thorlacius, H. (2008) Critical role of p38 mitogen-activated protein kinase signaling in septic lung injury. *Crit. Care Med.* **36**, 482–488
49. Behr, T. M., Nerurkar, S. S., Nelson, A. H., Coatney, R. W., Woods, T. N., Sulpizio, A., Chandra, S., Brooks, D. P., Kumar, S., Lee, J. C., Ohlstein, E. H., Angermann, C. E., Adams, J. L., Sisko, J., Sackner-Bernstein, J. D., and Willette, R. N. (2001) Hypertensive end-organ damage and premature mortality are p38 mitogen-activated protein kinase-dependent in a rat model of cardiac hypertrophy and dysfunction. *Circulation* **104**, 1292–1298
50. Klintman, D., Li, X., Santen, S., Schramm, R., Jeppsson, B., and Thorlacius, H. (2005) p38 mitogen-activated protein kinase-dependent chemokine production, leukocyte recruitment, and hepatocellular apoptosis in endotoxemic liver injury. *Ann. Surg.* **242**, 830–838, discussion 838–839
51. Badger, A. M., Griswold, D. E., Kapadia, R., Blake, S., Swift, B. A., Hoffman, S. J., Stroup, G. B., Webb, E., Rieman, D. J., Gowen, M., Boehm, J. C., Adams, J. L., and Lee, J. C. (2000) Disease-modifying activity of SB 242235, a selective inhibitor of p38 mitogen-activated protein kinase, in rat adjuvant-induced arthritis. *Arthritis Rheum.* **43**, 175–183
52. Cain, B. S., Meldrum, D. R., Dinarello, C. A., Meng, X., Joo, K. S., Banerjee, A., and Harken, A. H. (1999) Tumor necrosis factor-alpha and interleukin-1beta synergistically depress human myocardial function. *Crit. Care Med.* **27**, 1309–1318
53. Haudek, S. B., Spencer, E., Bryant, D. D., White, D. J., Maass, D., Horton, J. W., Chen, Z. J., and Giroir, B. P. (2001) Overexpression of cardiac I-kappaBalpha prevents endotoxin-induced myocardial dysfunction. *Am. J. Physiol. Heart Circ. Physiol.* **280**, H962–H968
54. Fisher, C. J. Jr., Agosti, J. M., Opal, S. M., Lowry, S. F., Balk, R. A., Sadoff, J. C., Abraham, E., Schein, R. M., and Benjamin, E.; The Soluble TNF Receptor Sepsis Study Group. (1996) Treatment of septic shock with the tumor necrosis factor receptor:Fc fusion protein. *N. Engl. J. Med.* **334**, 1697–1702
55. Abraham, E., Laterre, P. F., Garbino, J., Pingleton, S., Butler, T., Dugernier, T., Margolis, B., Kudsk, K., Zimmerli, W., Anderson, P., Reynaert, M., Lew, D., Lesslauer, W., Passe, S., Cooper, P., Burdeska, A., Modi, M., Leighton, A., Salgo, M., and van der Auwera, P.; Lenercept Study Group. (2001) Lenercept (p55 tumor necrosis factor receptor fusion protein) in severe sepsis and early septic shock: a randomized, double-blind, placebo-controlled, multicenter phase III trial with 1,342 patients. *Crit. Care Med.* **29**, 503–510
56. Pinsetta, F. R., Taft, C. A., and de Paula da Silva, C. H. (2014) Structure- and ligand-based drug design of novel p38-alpha MAPK inhibitors in the fight against the Alzheimer's disease. *J Biomol Struct Dyn* **32**, 1047–1063
57. Trunzer, K., Pavlick, A. C., Schuchter, L., Gonzalez, R., McArthur, G. A., Hutson, T. E., Moschos, S. J., Flaherty, K. T., Kim, K. B., Weber, J. S., Hersey, P., Long, G. V., Lawrence, D., Ott, P. A., Amaravadi, R. K., Lewis, K. D., Puzanov, I., Lo, R. S., Koehler, A., Kockx, M., Spleiss, O., Schell-Steven, A., Gilbert, H. N., Cockey, L., Bollag, G., Lee, R. J., Joe, A. K., Sosman, J. A., and Ribas, A. (2013) Pharmacodynamic effects and mechanisms of resistance to vemurafenib in patients with metastatic melanoma. *J. Clin. Oncol.* **31**, 1767–1774
58. Cattin, M. E., Muchir, A., and Bonne, G. (2013) 'State-of-the-heart' of cardiac laminopathies. *Curr. Opin. Cardiol.* **28**, 297–304

Received for publication February 20, 2017.
Accepted for publication May 15, 2017.